Electronic Supplementary Material (ESI) for Journal of Materials Chemistry C.

Supplementary Information

Harnessing low frequency-based energy using $K_{0.5}Na_{0.5}NbO_3$ (KNN) pigmented piezoelectric paint system

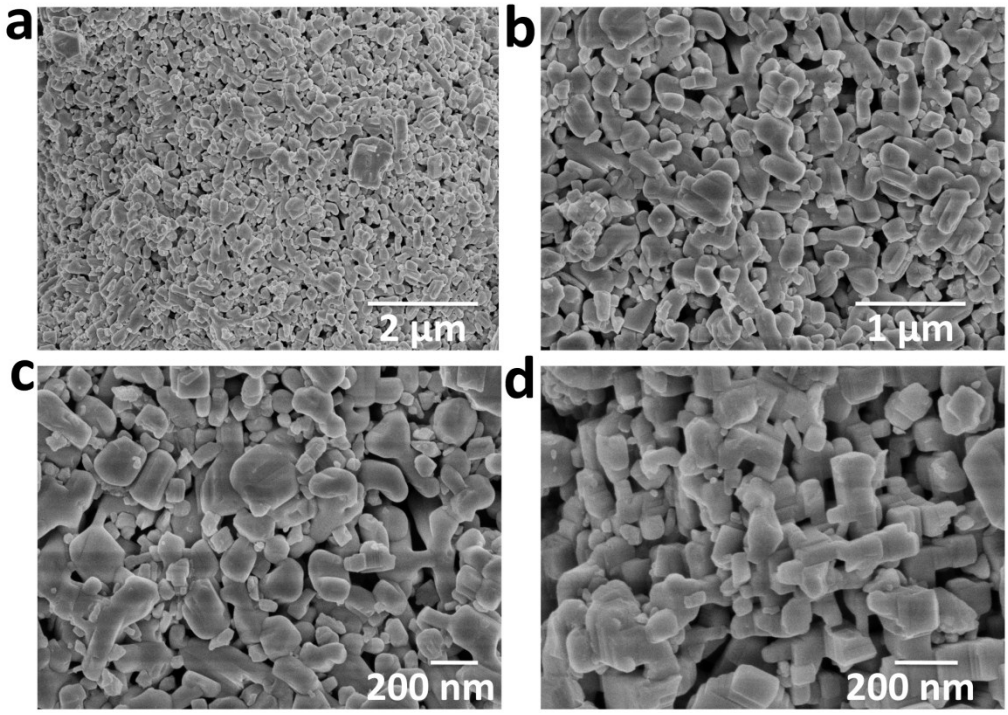

Figure S1. FESEM images at different scale rate (2 µm, 1 µm and 200 nm) of as-synthesized KNN nanoparticles calcinated at a temperature of at 850 °C for 10 h

Figure S2 shows the polarization (P) vs. electric field (E) hysteresis loop at a frequency of 1 Hz, confirming the ferroelectric property exhibited by $K_{0.5}Na_{0.5}NbO_3$ sample sintered for 2 h at 1120°C. The hysteresis loop at a drive voltage of 1 kV/cm, demonstrates the existence of polarization with a lossy capacitance nature of as-synthesized KNN pigment[1]. This kind of inflated behavior is mainly due to the contribution of leakage current which depends upon various factors. Firstly, the presence of oxygen vacancies adds up to high leakage current and secondly, there is a size and geometrical effect as the dimension of the material is lowered[2, 3]. The reduced grain size of prepared KNN (~ 300 nm) affects the polarization, leaving it unsaturated. Despite these factors, the sintered KNN nanomaterial possesses reasonable piezoelectric properties with remnant polarization (P_r) of ~ 99 μC/cm^2 and coercive fields (E_c) of ~ 820 V/cm which are higher than reported in the literature[2, 4]. A further improvement in piezoelectric properties can be achieved by reducing the leakage current through suitable doping mechanism and processing temperature[4].

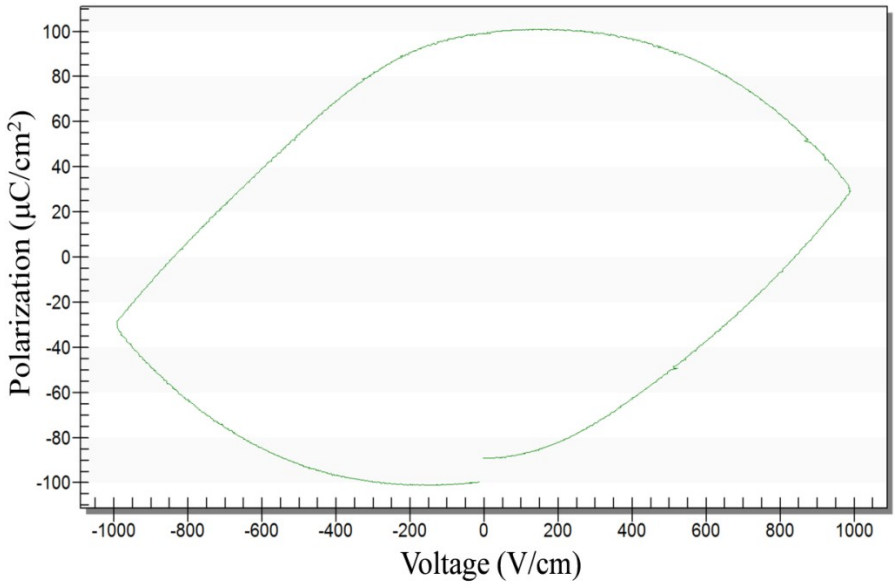

Figure S2. P-E hysteresis loop of as-prepared $K_{0.5}Na_{0.5}NbO_3$ sample sintered for 2 h at 1120°C

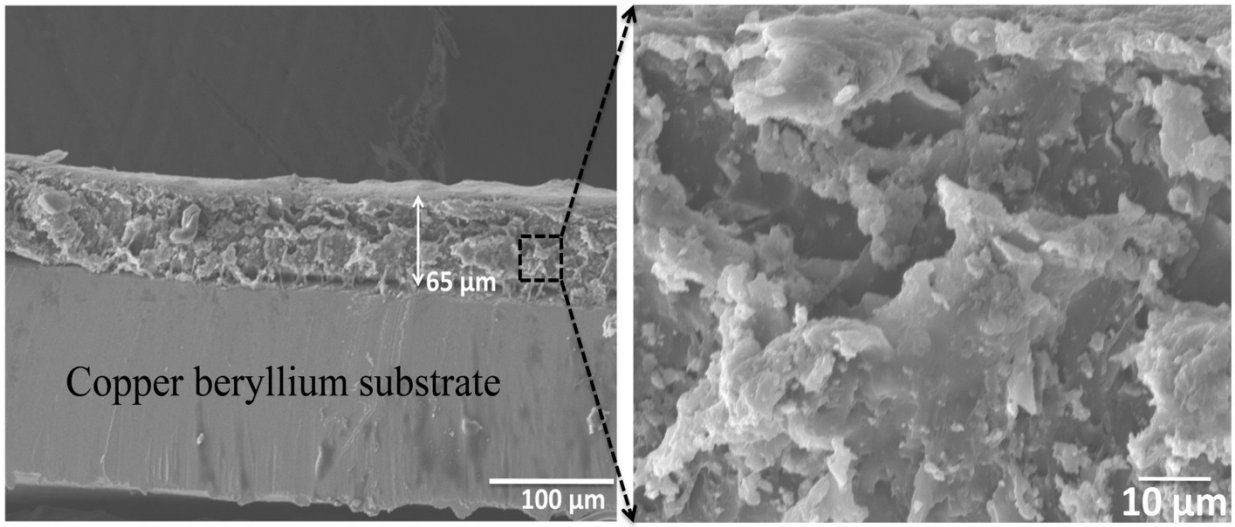

Figure S3. Cross-sectional FE-SEM analysis of KNN based piezoelectric paint coated on copper beryllium substrate.

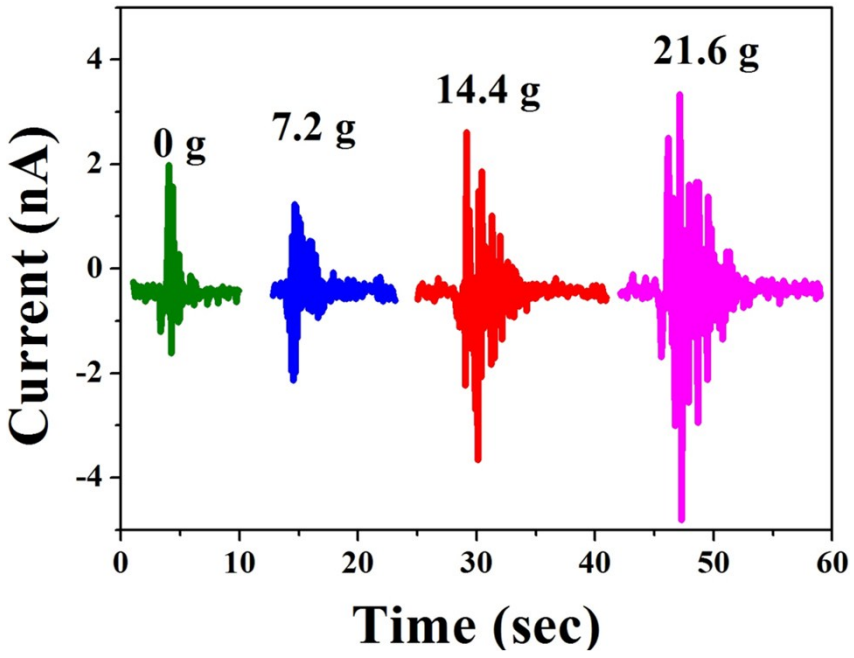

Figure S4. Piezoelectric current response as a function of increased proof mass ((m_p = 0, 7.2, 14.4 and 21.6 g)

Table: S1 Comparison on the cantilever configuration of proposed KNN based piezoelectric paint with other published reports.

Material	**Cantilever configuration**	**Dimension (mm)**	**m_p[a] (g)**	**V_{OC}[b] (V)**	**f_0[c] (Hz)**	**Ref**
PZT-5A	Bimorph	125 × 13.2 × 21.3 3	0.72	3.3	36	5
PZT	Bimorph	8 × 5 × 0.4	0.8	0.08	51	6
PZT	Bimorph	40 × 220 × 0.8	12	0.19 mW (P)	14.5	7
PZT-5A	Bimorph	90 × 40 × 24	-	2.47	-	8
PZT	Unimorph	11.5 × 12.7	0.7	0.32	60	9
PVDF	Unimorph	30 × 12.2 × 0.125	8600 kg/m^3	4.72	4 - 6	10
ZnO	Fiber	50 × 50	1	0.39 70 nA (I_{SC})	175	11
KNN	Unimorph	50 × 15	21.6	1.4 8 nA (I_{SC})	3.8	This work

[a] Proof mass; [b] Piezoelectric output voltage; [c] Resonant frequency

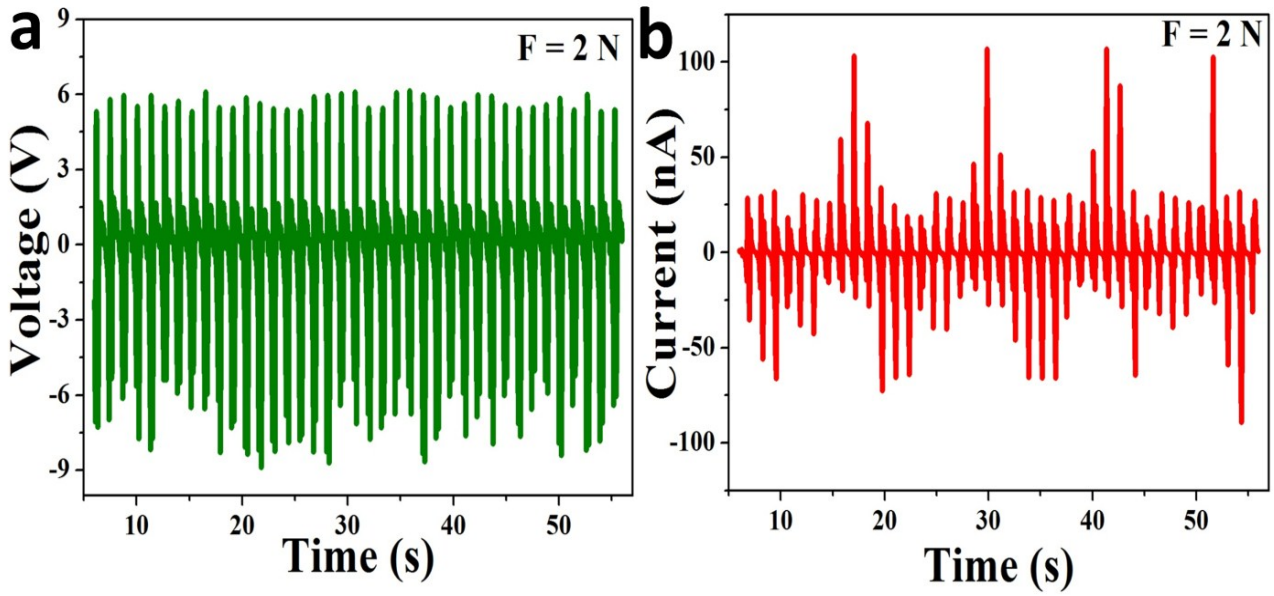

Figure S5. Piezoelectric performance of KNN based piezoelectric paint under a constant load of 2 N **(a)** Electrical output voltage (V_{OC}) **(b)** Electrical output current (I_{SC})

The reliability of the piezoelectric paint was examined under a constant mechanical load of 2 N (obtained by a linear motor shaft mass (2 kg) moving with an acceleration of 1 m/s^2). The piezoelectric paint generated a maximum electrical output of $V_{OC} \approx 12$ V and $I_{SC} \approx 70$ nA.

Table: S2 Comparison of energy harvesting ability of KNN paint with other published reports.

Material	**Area (cm)**	**Force**	**V_{OC}[a] (V)**	**I_{SC}[b] (A)**	**Ref**
$K_{0.5}Na_{0.5}NbO_3$/PDMS	2.5 × 4.5	Finger	0.17	4.48 n	12
$K_{0.6}Na_{0.4}NbO_3$ Nanorods	-	1 kgf	0.38	6.4	13
0.9525($K_{0.5}Na_{0.5}NbO_3$)-0.0475$LiTaO_3$/PDMS	2.1 × 1.7	140 N	53	15 μ	14
0.942($K_{0.480}Na0_{.535}$)NbO_3-0.058$LiNbO_3$/PDMS	3 × 3	0.33 % (strain)	12	1.2 μ	15
$K_{0.5}Na_{0.5}Nb_{0.995}Mn_{0.005}O_3$/Silk solution	-	500 μN	1.8	0.1 μ	16
0.96($K_{0.48}Na_{0.52}$)($Nb_{0.95}Sb_{0.05}$)O_3– 0.04$Bi_{0.5}$($Na_{0.82}K_{0.18}$)0.5ZrO_3/PDMS	2 × 2	-	10	-	17
$K_{0.5}Na_{0.5}NbO_3$/Alkyd (piezoelectric paint)	5 × 1.5	2 N	12	70 n	This work

[a] Piezoelectric output voltage; [b] Piezoelectric output current

References:

1 Z. Wang, Y. Hu, W. Wang, D. Zhou, Y. Wang and H. Gu, *Integrated Ferroelectrics*, 2013, **42**, 24–30.

2 D. Zhou, H. Gu, Y. Hu, H. Tian, Z. Wang, Z. Qian and Y. Wang, *J. App. Phys*., 2011, **109**, 114104.

3 M. U. Farooq, J. G. Fisher, J. H. Kim, and D. Zhang, *J. Ceramic Proc. Res.,* 2016, **17**, 304-312.

4 P. Zhao, B. P. Zhang and J. F. Li, *App. Phys. Letters,* 2007, **90**, 242909.

5 L. Dhakar, H. Liu, F. E. H. Tay and C. Lee, *Sensors Actuators A. Phys.*, 2013, **199**, 344–352.

6 H. Liu, C. Lee, T. Kobayashi, C. J. Tay and C. Quan, *Sensors Actuators A. Phys.*, 2012, **186**, 242–248.

7 X. Jiang, Y. Li, J. Li, J. Wang and J. Yao, *J. Renewable Sustainable Energy*, 2014, **6**, 1-16.

8 S Wei, H. Hu and S. He, *Smart Mater. Struct.* , 2013, **22**, 105020-105028.

9 E. Fernandes, S. Zarabi, H. Debéda, C. Lucat, *J. Physics: Conference Series*, 2016, **773,** 012109.

10 X. Ma, A. Wilson, C. D. Rahn and S. Trolier-mckinstry, *J. Vibration and Acoustics,* 2016, **138,** 1–9.

11 M. H. Malakooti, B. A. Patterson, H. S. Hwang and H. A. Sodano, *Energy Environ. Sci.***,** 2016, **9**, 634-643.

12 Y. Zhuang, Z. Xu, F. Li, Z. Liao and W. Liu, *J. Alloys Compd.*, 2015, **629**, 113–117.

13 P. G. Kang, B. K. Yun, K. D. Sung, T. K. Lee, M. Lee, N. Lee, S. H. Oh, W. Jo, H. J. Seog, C. W. Ahn, I. W. Kim and J. H. Jung, *RSC Adv.,* 2014, **4**, 29799–29805.

14 Q. Xue, Z. Wang, H. Tian, Y. Huan, Q. Xie, Y. Yang, D. Xie, C. Li, Y. Shu and T. Ren, *AIP Advances*, 2015, **5**, 017102-7.

15 C. K. Jeong, K. Park, J. Ryu, G. Hwang and K. J. Lee, *Adv. Funct. Mater.* **,** 2014, 1–10.

16 K. N. Kim, J. Chun, S. A. Chae, C. W. Ahn, I. W. Kim, S. Kim, Z. L. Wang and J. M. Baik, *Nano Energy*, 2015, **14**, 87–94.

17 R. Zhu, J. Jiang, Z. Wang, Z. Cheng and H. Kimura, *RSC Adv.*, 2016, **6**, 66451–66456.